

# Oscillations in Josephson transmission line stimulated by load in the presence of noise

A. L. Pankratov, E. V. Pankratova, V. A. Shamporov, and S. V. Shitov

Citation: *Appl. Phys. Lett.* **110**, 112601 (2017); doi: 10.1063/1.4978514

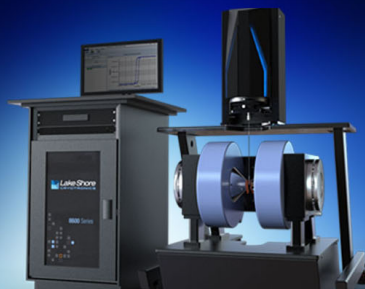
View online: <http://dx.doi.org/10.1063/1.4978514>

View Table of Contents: <http://aip.scitation.org/toc/apl/110/11>

Published by the [American Institute of Physics](#)

---

---



**NEW 8600 Series VSM**

For fast, highly sensitive  
measurement performance

**LEARN MORE** 

# Oscillations in Josephson transmission line stimulated by load in the presence of noise

A. L. Pankratov,<sup>1,2,3</sup> E. V. Pankratova,<sup>3</sup> V. A. Shamporov,<sup>1,2,3</sup> and S. V. Shitov<sup>4,5</sup>

<sup>1</sup>*Institute for Physics of Microstructures of RAS, GSP-105, Nizhny Novgorod 603950, Russia*

<sup>2</sup>*CCN, Nizhny Novgorod State Technical University n.a. R.E. Alexeyev, Nizhny Novgorod 603950, Russia*

<sup>3</sup>*N.I. Lobachevsky State University of Nizhni Novgorod, Nizhny Novgorod 603950, Russia*

<sup>4</sup>*Institute of Radio-engineering and Electronics of RAS, Moscow 125009, Russia*

<sup>5</sup>*LSM, National University of Science and Technology "MISIS," Moscow 119049, Russia*

(Received 27 November 2016; accepted 24 February 2017; published online 14 March 2017)

The joint action of the matching to a common RC-load and thermal noise on the spectral properties of parallel Josephson junction array is studied. It is demonstrated that proper matching suppresses the chaotic dynamics of the system. The efficiency of radiation is found to be highest within a limited frequency band, which corresponds to transformation of the shuttle soliton oscillating regime into the linear wave resonance synchronization mode. In this frequency band the spectral linewidth agrees well with a double of the linewidth for a shuttle fluxon oscillator, divided by a number of the oscillators in the array. When the oscillations demonstrate strong amplitude modulation, the linewidth increases roughly by a factor of five compared with theoretical linewidth formula. Published by AIP Publishing. [<http://dx.doi.org/10.1063/1.4978514>]

The dynamics of systems where the nonlinear active elements are mutually coupled through additional external media can demonstrate surprising properties of collective behavior. Such coupling is widely spread in nature and technology and describes, for example, vibrations of a common base supporting oscillating mechanical systems,<sup>1–3</sup> electromagnetic field interacting with cold atoms,<sup>4</sup> common dynamic environment indirectly linking the electronic circuits,<sup>5</sup> etc. Regimes observed in such systems are highly diverse, varying from oscillation quenching to a multitude of synchronous regimes.<sup>1,5,6</sup> However, the results of deterministic modeling and behavior of a real system in the presence of fluctuations can be radically different, e.g., accounting for environmental noise can modify the dynamics via new mechanisms;<sup>7</sup> also recently several noise-induced effects have been predicted.<sup>8–10</sup> For these reasons, the investigation of joint effects of noise and a common load on dynamics of complex networks is of growing interest.

One of the important tasks is development of a high-efficient Josephson oscillator loaded with an antenna or with a waveguide, while unavoidable fluctuations are not negligible. The increasing interest to the Josephson effect is nowadays associated with its THz potential for heterodyne detection.<sup>11</sup> Since the radiation power of a single Josephson junction (JJ) is rather weak (does not exceed  $P = I_c V_c \cdot 10^{-8} W$ ), there is motivation for development and study of synchronous arrays of Josephson junctions (JJAs),<sup>12–19</sup> aiming to larger radiation power. The efficient yet compact serial-parallel 2-D JJA was fabricated and studied as described in Ref. 16. The remarkably high efficiency of radiation and a clear threshold of generation in such array have been discussed in a few papers, but are not completely understood yet. The authors of Ref. 16 have suggested the internal cell resonance to be responsible for the oscillating frequency. In Refs. 18 and 19 it has been qualitatively shown that threshold effect can be observed if a JJA is coupled to a high-Q cavity load. But, a real application, e.g.,

Ref. 20, needs frequency tunability that is associated with low-Q regimes. To address this problem, an RC-load must be placed at one end of the chain.<sup>16</sup> However, due to the distributed nature of a JJA (e.g., Josephson transmission line, JTL), the damping leads to a condition that not all JJs in the chain are coupled equally to the load. Thus, we may state lack of understanding in synchronism for practicable JJA. In the present Letter we consider a complex dynamics of JJA defined by its load in the presence of thermal noise; we argue that similar threshold in radiation power and high efficiency as in Ref. 16 can be observed in a relatively simple parallel (ladder-type) JJA damped with RC-load. Such effects have also crucial importance in layered superconductors,<sup>11</sup> which are mostly treated theoretically in an unmatched case.<sup>21,22</sup>

Our numerical study is performed in the frame of the Frenkel–Kontorova model<sup>23</sup>

$$\ddot{\phi}_j + \alpha \dot{\phi}_j + \sin \phi_j = i_{dc} + i_f(t) + \varepsilon(\phi_{j-1} - 2\phi_j + \phi_{j+1}), \quad (1)$$

which has a broad variety of mechanical, chemical, biological, and physical applications, including Josephson-junctions-based digital circuits<sup>24</sup> and ballistic detectors.<sup>25,26</sup> In our case, Eq. (1) describes dynamics of JJA shown in Fig. 1, where crosses denote JJs with their internal capacitance, resistance, and nonlinear inductance,  $\phi_j$  is the phase of the  $j$ -th JJ,  $\alpha$  is

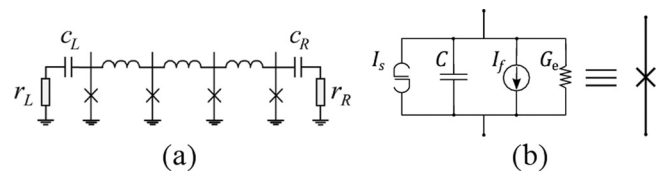


FIG. 1. (a) General scheme of JJA comprising inductively coupled Josephson junctions (JJs, denoted as crosses); terminals of JJA are RC-loaded with  $r_L$  and  $r_R$ ; all JJ are biased at dc in parallel, forming a Josephson transmission line (JTL). (b) Equivalent electrical circuit for a Josephson junction (JJ).

the damping, and the coupling parameter  $\epsilon = 1/l$  is the inverse inductance between JJs. This inductance-related parameter defines the spatial scale of the JJA via normalization  $\Delta x = \sqrt{l}$ , where the cell size  $\Delta x$  is expressed in units of Josephson length  $\lambda_J$ . Each JJ (each cell-oscillator) is biased by the dc current  $i_{dc}$  and subjected to fluctuations  $i_f(t)$ , which is assumed to be white Gaussian noise with the dimensionless intensity  $\gamma$ :  $\langle i_f(t)i_f(t+\tau) \rangle = 2\alpha\gamma\delta(\tau)$ . We consider the JJ chain terminated with the RC-load<sup>27,28</sup> under the condition  $di_R/dt = -i_R/r_{RCR} + \dot{\phi}_n(t)/r_R$ , where  $i_R(t)$  is the alternating current through the right load and  $r_R$  and  $c_R$  are the dimensionless resistance and capacitance, respectively; similar equation can be written for the left load ( $r_L$  and  $c_L$ ). The bias current  $i_{dc}$  is injected evenly as shown in Fig. 1(a). Note that the Josephson junctions in the array are protected from unequal dc voltage even in case of spread of their parameters, since they all are connected in parallel, which ensures the same oscillating frequency for all cells.

It is known from Ref. 16 that oscillations in underdamped JJA are manifested as steps at I-V curve (IVC). Considering the radiation efficiency of JJA, we calculate spectra at the output in terms of power and linewidth at different steps of IVC. The system (1) has been solved numerically for the following parameters relevant to published experiments:  $\alpha = 0.03$ ,  $\epsilon = 4.41$  and number of junctions  $N = 20$ . The calculated IVC is present in Fig. 2 that is time averaged voltage  $v = d\phi(t)/dt$  versus the bias current  $i_{dc}$ ; noiseless condition ( $\gamma = 0$ ) is used; coupling is weak at the left end ( $r_L = 30$ ,  $c_L = 100$ ), and the right end is unmatched ( $r_R = 100$ ,  $c_R = 100$ ). Load capacitances are sufficiently large allowing for transmission at all frequencies of interest. For small currents  $i_{dc} \rightarrow 0$  the system remains in the superconducting state. At large currents, approaching the critical value  $i_c = 1$ , namely from  $i_{dc} > 0.6$ , the behavior is ohmic, i.e., the voltage is proportional to the characteristic resistance  $v = i_{dc}/\alpha$ .

The first step of the IVC ( $v_1$ ) corresponds to a single soliton moving along the chain.<sup>15</sup> The second and the third steps

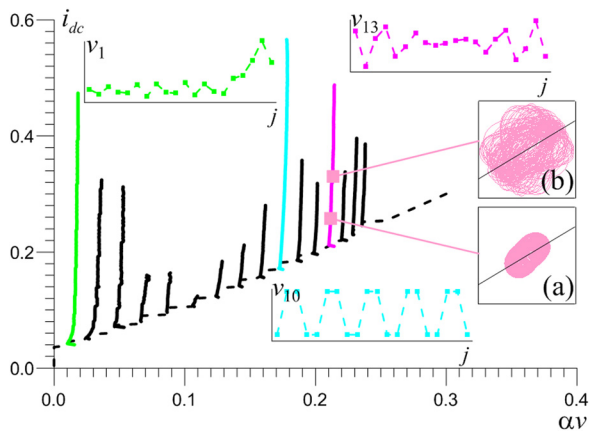


FIG. 2. I-V characteristics (IVCs) of JJA for weakly coupled load  $r_L = 30$ ; the steep solid curves (steps correspond to different regimes of excitation) are so-called direct-path (growing current) IVCs; the dashed curve corresponds to return-path IVC. Insets: the voltage distribution  $v_k = d\phi_j(t)/dt$  (for particular steps:  $k = 1, 10, 13$ ) versus the junction number,  $j$ ; two phase portrait  $(v_i, v_j)$ -projections for unmatched case  $c_L = c_R = 0$  at: (a)  $i_{dc} = 0.26$ , (b)  $i_{dc} = 0.33$ .

( $v_2$  and  $v_3$ ) correspond to two and three solitons. At 4th and 5th steps the behavior appears chaotic; the reason may be either destructive interference of linear waves or a combination of effects of restricted length of JJA ( $\sim 10\lambda_J$ ) and its discreteness. One can also observe the minor steps at IVCs due to Cherenkov radiation of moving solitons.<sup>15,26,29–31</sup> At low currents of high-order steps the standing waves develop (inset in Fig. 2 for  $v_{10}(j)$ ). At 10th step, the amplitude is significantly larger than for the first three steps. It is worth to note that, at the top of 12th and higher-order steps, the transition to chaos is observed in case of the completely unmatched load ( $c_L = c_R = 0$ ) meaning an open circuit. The analysis of the spectrum evolution on bias current  $i_{dc}$  (not shown) confirms destabilization of the stable quasi-periodic oscillations (inset (a) in Fig. 2) leading to the emergence of a chaotic attracting set (inset (b) in Fig. 2).<sup>32</sup> But this chaotic behavior disappears if some load is present. Even for weak match ( $r_L = 30$  in Fig. 2), at the tops of the high-order steps of IVCs the stable quasi-periodic motion will develop (see below).

If a matched load is placed at one end of the chain ( $r_L = 2$ ,  $c_L = 100$ , while  $r_R = 100$ ,  $c_R = 100$ ), the IVCs for higher steps (8th–16th, shown as thinner, colored curves in Fig. 3) change drastically. As seen from Fig. 3, the role of proper load is crucial: all steps below 8th disappear (see the jump from zero voltage to the 8th step) meaning that a few-soliton train cannot exist being absorbed by the load. Moreover, the high-order steps become taller in terms of  $i_{dc}$  and the dynamics at their tops changes significantly. The amplitude modulation regimes shift to larger  $i_{dc}$ , and the chaotic regimes do not evolve (the oscillations become more regular in comparison with unmatched case). The phase portrait projection calculated for zero noise intensity  $\gamma = 0$  at 12th step for bias  $i_{dc} = 0.41$  (inset (a) in Fig. 3) demonstrates the limit cycle corresponding to a purely periodical oscillations; the regimes with amplitude modulation observed at 12th (for  $i_{dc} = 0.49$ ) and 13th (for  $i_{dc} = 0.41$ ) steps are depicted in Fig. 3 within the insets (b) and (c), respectively. The inset (d) in Fig. 3 illustrates vanishing of the amplitude

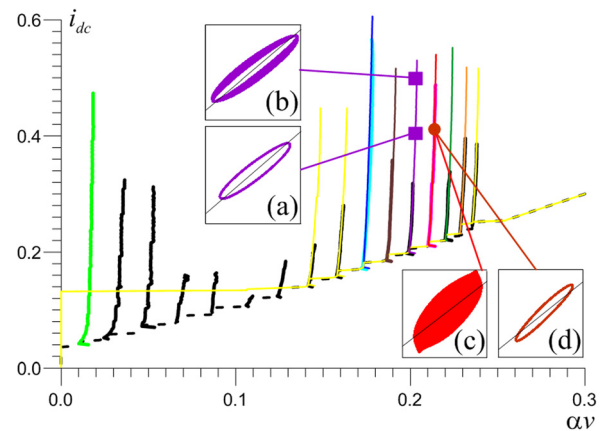


FIG. 3. Comparison of I-V curves for well matched JJ array. Thin yellow and colored curves correspond to direct-path and return IVCs for  $r_L = 2$ , while other curves are the same as in Fig. 2. Insets: phase portrait  $(v_i, v_j)$ -projections: (a) pure periodic wave at  $i_{dc} = 0.41$  and (b) amplitude modulation at higher  $i_{dc} = 0.49$ , both for  $r_L = 2$  at 12th step; (c) deep amplitude modulation at  $r_L = 2$ ; and (d) no modulation for ideal match  $r_L = r_R = 1$ , both for  $i_{dc} = 0.41$  at 13th step.

modulation due to the perfect match,  $r_L = r_R = 1$ . For low noise  $\gamma \leq 0.1$ , the IVC step heights are roughly the same as for the noiseless case,  $\gamma = 0$  (data not shown). The power transmitted to the left load can be computed from spectral density of signal at the leftmost JJ as the integral<sup>27,33</sup>

$$P = \frac{1}{2\pi} \int_{\omega_0 - \delta\omega}^{\omega_0 + \delta\omega} \frac{S(\omega)}{r_L(1 + 1/(r_L c_L \omega)^2)} d\omega,$$

where  $\omega_0$  is the central frequency of the main spectral peak of  $S(\omega)$ , and  $\delta\omega$  is chosen so that the main peak and a number of satellites (which can fit into the receiver bandwidth) are enclosed within the integration interval; for shuttle soliton regimes with dense spectrum of harmonics (i.e., at the lower steps of the IVC), the power is integrated across several adjacent peaks. The implicit numerical scheme for the solution of Eq. (1) with noise has been first used and tested in Ref. 34.

The radiation power at the left load versus bias current is shown in Fig. 4(a). For weakly matched load  $r_L = 30$  and noise intensity  $\gamma = 0.05$  this regime resembles the experiment:<sup>16</sup> the power at first six steps is rather weak; it does not grow until the bias is reaching high-order steps (data for steps 1, 3, and 10 are shown by symbols). For well matched RC-load  $r_L = 2$  the oscillation power grows linearly with the increase of bias current  $i_{dc}$ , as in experiments with flux-flow oscillators.<sup>20</sup> Dependent on the step number, the power varies twice throughout steps 8–15, reaching its maximum at the 10th step. Note that synchronization of JJ clusters results in power of several orders of magnitude larger than for perfect in-phase synchronization of all junctions at the resistive branch of the IVC. This can be explained with the theory of ac circuits. The resistive branch of IVC corresponds to capacitive embedding impedance of the JJs, which are nearly shorted at high frequencies. Resonant phenomena may create a condition, which nearly cancels this capacitive impedance, leading to dc steps and manifesting improvement in the radiation potential.

One can find the conversion ratio of ac to dc power,  $\eta$ , see Fig. 4(b). Note that for the 10th step with a matched load we get nearly the same efficiency as in experiment.<sup>16</sup> Such increase in power is accompanying the transition from zero-field steps to the resonant Fiske modes (see IVCs at Figs. 2 and 3). Such transition is characterized by the change of

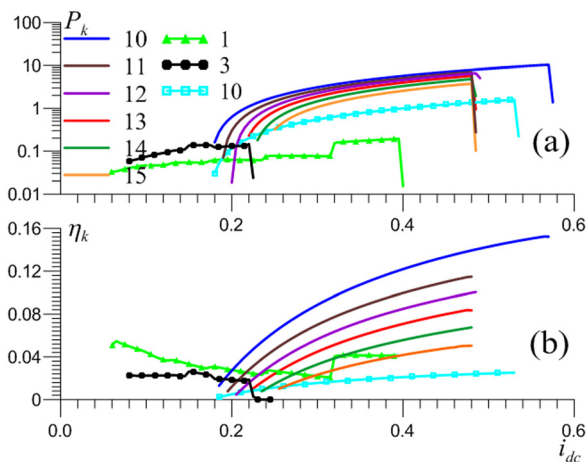


FIG. 4. Variation of (a) the radiation power at the left load  $P_k$  and (b) the radiation efficiency  $\eta_k$  vs bias current for  $k$ -th step of IVC; solid curves for  $r_L = 2$ ,  $r_R = 100$ , and curves with symbols for  $r_L = 30$ ,  $r_R = 100$ .

intervals between steps from almost  $3\pi/L$  at first steps to  $2\pi/L$  around 10th step and to  $\pi/L$  around 15th step. This effect can be explained by the constructive interference of linear waves in JJA formed by partial reflection from its unmatched boundaries (loads).

The maxima of radiation power  $P_k$  absorbed by loads of JJA vs bias voltage are plotted in Fig. 5 for a number of key parameters. One can see that improvement in match at one end may increase the power without shifting the optimal frequency range, while loads at both ends lead to the shift of maximum power to higher frequencies. In the latter case one should take into account that power is extracted from both ends of JJA, so the total power is twice of that presented in Fig. 5. This can be explained with electrical length at resonance: unloaded end corresponds to odd-number of quarter-wavelength of the JJA, but both loaded ends correspond to half-wavelength that leads to higher resonant frequency. The maximal efficiency reaches 15% for the loads  $r_L = 2$ ,  $r_R = 100$ . Increasing the number of junctions in the chain to  $N = 30$ , while its length is fixed, shifts the optimal frequency range up by a factor of 1.5. At the same time the radiation power increases, but efficiency  $\eta_k$  drops down. Increasing both the number of junctions  $N = 40$  and length  $L = 20\lambda_J$  allows for keeping the coupling parameter  $\epsilon$  the same as for  $N = 20$  and length  $L = 10\lambda_J$ . In this case the radiation efficiency grows at the optimum point, but decreases at higher frequencies. This proves that the optimum regime is a result of interference of linear waves related to both JJA length and reflection from terminal loads.

The curves of spectral linewidth at zero field steps are shown in Fig. 6 versus bias current  $i_{dc}$ , with the values by about two or three orders of magnitude smaller than at flux-flow steps<sup>33,35</sup> at the same damping  $\alpha$ , which requires much higher spectral resolution. The smaller linewidth in zero-field regime is presumably due to smaller dissipation, resulting in much smaller differential resistance. Comparing the calculated linewidth with the analytical formulas for the single JJ<sup>36</sup> and the shuttle fluxon oscillator,<sup>37</sup> one can see that for the 10th and 12th steps the linewidth can fit the analytical result<sup>37</sup> if multiplied by a factor of 2 and divided by the number of junctions  $N$

$$\Delta f = \alpha \gamma r_d^2 / N. \quad (2)$$

The factor  $2/N$  can be attributed to the fact that we consider not a single-fluxon regime, but a regime of mixed

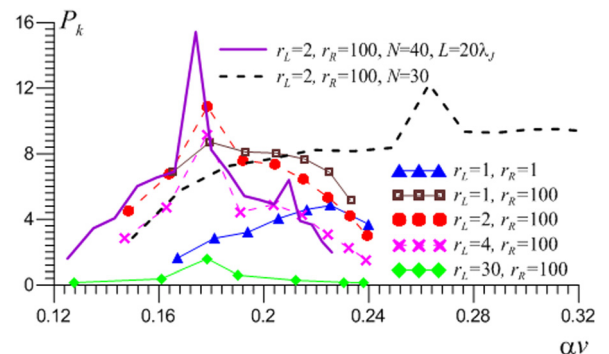


FIG. 5. Radiation power  $P_k$  vs voltage for various RC loads and number of junctions in JJA with length  $L = 10\lambda_J$  unless another length is specified.

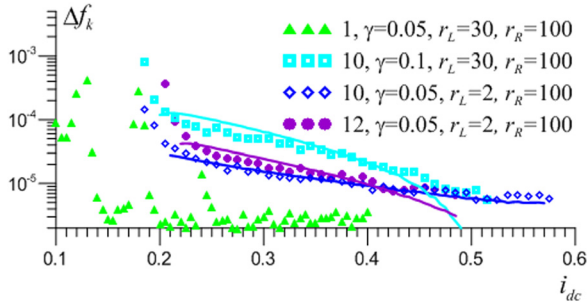


FIG. 6. Spectral linewidth  $\Delta f_k$  vs bias current  $i_{dc}$  for  $k$ -th step of IVC; solid curves denote theoretical relation (2).

traveling and standing waves. Comparison of calculated and theoretical linewidth at the first step is out of our present computational capabilities due to sharp Cherenkov steps at the IVC, requiring extreme calculation accuracy at low differential resistance  $r_d$ . As seen from Fig. 6, at the top of the 10th and 12th steps the deviation of the calculated linewidth from theory (2) increases. This can be explained by amplitude modulation at the step tops (inset b in Fig. 3) that, in the absence of noise, leads to zero linewidth.<sup>38</sup> However, the presence of thermal noise causes the diffusion of phase, which interplays with the amplitude modulation and leads to the additional linewidth increase, thus deviating from Eq. (2). For the 13th step the linewidth increases up to a factor of five in comparison with theory (see Fig. 7 and supplementary material for details). For  $i_{dc} = 0.35$ , regular oscillation regimes are observed, and the shape of spectral line is perfectly Lorentzian, see Fig. 8(a). However, for  $i_{dc} = 0.41$  at the same step the spectral peak becomes asymmetrical (see Fig. 8(b)), which confirms the presence of the mutual effect of amplitude and phase fluctuations,<sup>38</sup> leading to the linewidth increase. Improving the matching ( $r_L = r_R = 1$ ) suppresses the amplitude modulation and the linewidth restores back to Eq. (2). The linewidth for JJAs having the same length but different number of junctions  $N$  is presented as inset of Fig. 7 for the 10th step ( $r_L = 2, r_R = 100$ ). Again, Eq. (2) gives good agreement with numerical results, since for the 10th step regular generation develops in a wide range of bias.

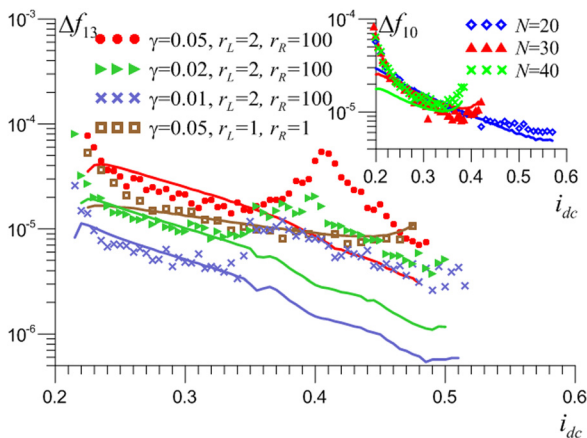


FIG. 7. Spectral linewidth  $\Delta f_{13}$  vs bias current  $i_{dc}$  for 13th step of IVC for various values of  $\gamma$  and load resistance. Inset: spectral linewidth versus bias current for 10th step of IVC for various number of junctions in the chain; solid curves denote theory (2),  $\gamma = 0.05, r_L = 2, r_R = 100$ .

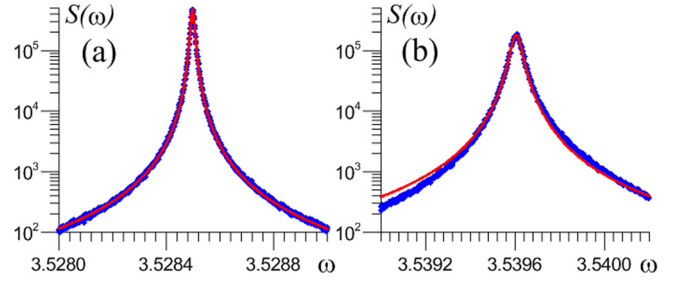


FIG. 8. The main peak of power spectral density at 13th step,  $r_L = 2, r_R = 100, \gamma = 0.05$ , symbols—computer simulations, and solid curve—Lorentzian fit: (a) for  $i_{dc} = 0.35$  a regular oscillation regime leads to perfectly Lorentzian shape; (b) for  $i_{dc} = 0.41$ , where amplitude modulation interplays with phase diffusion, the asymmetry of spectral peak is observed.

In the present paper we show that the threshold of radiation power and high efficiency of radiation can be observed in a simple parallel (ladder-type) JJ array with an RC load taken into account. We have demonstrated that the most efficient radiation can be anticipated within the frequency range that corresponds to transformation of the shuttle soliton oscillating regime into the linear wave resonance synchronization mode (i.e., from zero field steps into the Fiske steps at the IV-curve of the RC-loaded JJA, respectively). While we have considered the RC-load equally matched for all frequencies, in practice match is a design parameter achievable only within limited frequency range, so the observed threshold of radiation power can be magnified. In case of an optimum RC load, the radiation power is expected to reach 15% of the total dc power. Remarkably, for regular oscillation regimes at the high-order resonant steps, the linewidth agrees well with the half of theoretical value for a short Josephson junction<sup>36</sup> and a double for a shuttle fluxon oscillator,<sup>37</sup> divided by a number of the junctions in the chain. If the oscillations demonstrate strong amplitude modulation, it leads to increase of the linewidth by a factor of five in comparison with the theory.

See supplementary material for description of the mutual effect of amplitude and phase fluctuations.

We wish to thank V. Krasnov and M. Fistul for comments and suggestions. This work is supported by RFBR (Project Nos. 14-02-31727 and 15-02-05869), by Russian Ministry of Science (Project Nos. 11.G34.31.0062, 14.740.12.0845, and 3.2054.2014/K), by NUST MISiS Grant No. K2-2016-051 and Lobachevsky NNSU Grant No. 02.B.49.21.0003.

<sup>1</sup>M. Bennett, M. Schatz, H. Rockwood, and K. Wiesenfeld, *Proc. R. Soc. London, A* **458**, 563 (2002).

<sup>2</sup>E. V. Pankratova and V. N. Belykh, *Phys. Lett. A* **376**, 3076 (2012).

<sup>3</sup>S. H. Strogatz, D. M. Abrams, A. McRobie, B. Eckhardt, and E. Ott, *Nature* **438**, 43 (2005).

<sup>4</sup>J. Javaloyes, M. Perrin, and A. Politi, *Phys. Rev. E* **78**, 011108 (2008).

<sup>5</sup>R. Suresh, K. Srinivasan, D. V. Senthilkumar, K. Murali, M. Lakshmanan, and J. Kurths, *Int. J. Bifurcation Chaos* **24**, 1450067 (2014).

<sup>6</sup>V. Resmi, G. Ambika, R. E. Amritkar, and G. Rangarajan, *Phys. Rev. E* **85**, 046211 (2012).

<sup>7</sup>E. V. Pankratova and V. N. Belykh, *Eur. Phys. J.: Spec. Top.* **222**, 2509 (2013).

<sup>8</sup>A. L. Pankratov, *Phys. Rev. B* **68**, 024503 (2003).

- <sup>9</sup>A. L. Pankratov and B. Spagnolo, *Phys. Rev. Lett.* **93**, 177001 (2004); A. V. Gordeeva, A. L. Pankratov, and B. Spagnolo, *Int. J. Bifurcation Chaos* **18**, 2825 (2008).
- <sup>10</sup>K. G. Fedorov and A. L. Pankratov, *Phys. Rev. Lett.* **103**, 260601 (2009); G. Augello, D. Valenti, A. L. Pankratov, and B. Spagnolo, *Eur. Phys. J. B* **70**, 145 (2009); D. Valenti, C. Guarcello, and B. Spagnolo, *Phys. Rev. B* **89**, 214510 (2014).
- <sup>11</sup>U. Welp, K. Kadowaki, and R. Kleiner, *Nat. Photonics* **7**, 702 (2013).
- <sup>12</sup>A. K. Jain, K. K. Likharev, J. E. Lukens, and J. E. Sauvageau, *Phys. Rep.* **109**(6), 309 (1984).
- <sup>13</sup>S. G. Lachenmann, G. Filatrella, A. V. Ustinov, T. Doderer, N. Kirchmann, D. Quenter, R. P. Huebener, J. Niemeyer, and R. Pöpel, *J. Appl. Phys.* **77**, 2598 (1995).
- <sup>14</sup>P. A. A. Booi and S. P. Benz, *Appl. Phys. Lett.* **68**, 3799 (1996).
- <sup>15</sup>A. V. Ustinov, B. A. Malomed, and S. Sakai, *Phys. Rev. B* **57**, 11691 (1998).
- <sup>16</sup>P. Barbara, A. B. Cawthorne, S. V. Shitov, and C. J. Lobb, *Phys. Rev. Lett.* **82**, 1963 (1999).
- <sup>17</sup>D. Abraimov, P. Caputo, G. Filatrella, M. V. Fistul, G. Yu. Logvenov, and A. V. Ustinov, *Phys. Rev. Lett.* **83**, 5354 (1999).
- <sup>18</sup>G. Filatrella, N. F. Pedersen, and K. Wiesenfeld, *Phys. Rev. E* **61**, 2513 (2000); *IEEE TAS* **11**, 1184 (2001).
- <sup>19</sup>G. Filatrella, B. Straughn, and P. Barbara, *J. Appl. Phys.* **90**, 5675 (2001).
- <sup>20</sup>V. P. Koshelets and S. V. Shitov, *Supercond. Sci. Technol.* **13**, R53 (2000).
- <sup>21</sup>A. E. Koshelev, *Phys. Rev. B* **78**, 174509 (2008); S.-Z. Lin and A. E. Koshelev, *Phys. Rev. B* **87**, 214511 (2013).
- <sup>22</sup>V. E. Grishin and L. A. Muravey, *IEEE Trans. Appl. Supercond.* **21**, 3075 (2011); V. E. Grishin, L. A. Muravey, and V. A. Cherenkov, *ibid.* **21**, 3079 (2011).
- <sup>23</sup>Y. S. Kivshar and B. A. Malomed, *Rev. Mod. Phys.* **61**, 763 (1989).
- <sup>24</sup>K. K. Likharev and V. K. Semenov, *IEEE Trans. Appl. Supercond.* **1**, 3 (1991).
- <sup>25</sup>V. K. Semenov and D. V. Averin, *IEEE Trans. Appl. Supercond.* **13**, 960 (2003).
- <sup>26</sup>I. I. Soloviev, N. V. Klenov, A. L. Pankratov, E. Il'ichev, and L. S. Kuzmin, *Phys. Rev. E* **87**, 060901(R) (2013).
- <sup>27</sup>C. Soriano, G. Costabile, and R. D. Parmentier, *Supercond. Sci. Technol.* **9**, 578 (1996).
- <sup>28</sup>A. L. Pankratov, A. S. Sobolev, V. P. Koshelets, and J. Mygind, *Phys. Rev. B* **75**, 184516 (2007).
- <sup>29</sup>A. V. Ustinov, M. Cirillo, and B. A. Malomed, *Phys. Rev. B* **47**, 8357 (1993).
- <sup>30</sup>A. V. Ustinov, M. Cirillo, B. H. Larsen, V. A. Oboznov, P. Carelli, and G. Rotoli, *Phys. Rev. B* **51**, 3081 (1995).
- <sup>31</sup>O. M. Braun, B. Hu, and A. Zeltser, *Phys. Rev. E* **62**, 4235 (2000).
- <sup>32</sup>V. S. Anishchenko, V. Astakhov, A. Neiman, T. Vadivasova, and L. Schimansky-Geier, *Nonlinear Dynamics of Chaotic and Stochastic Systems: Tutorial and Modern Developments* (Springer Science & Business Media, 2007).
- <sup>33</sup>A. L. Pankratov, *Appl. Phys. Lett.* **92**, 082504 (2008).
- <sup>34</sup>K. G. Fedorov and A. L. Pankratov, *J. Commun. Technol. Electron.* **52**, 104–108 (2007).
- <sup>35</sup>A. L. Pankratov, *Phys. Rev. B* **78**, 024515 (2008).
- <sup>36</sup>J. Dahm, A. Denestein, D. N. Langenberg, W. H. Parker, D. Rogovin, and D. J. Scalapino, *Phys. Rev. Lett.* **22**, 1416 (1969).
- <sup>37</sup>E. Joergensen, V. P. Koshelets, R. Monaco, J. Mygind, M. R. Samuelsen, and M. Salerno, *Phys. Rev. Lett.* **49**, 1093 (1982).
- <sup>38</sup>A. N. Malakhov, *Fluctuations in Autooscillating Systems* (Science, Moscow, 1968) (in Russian).